I3S 2021

sciforum

Proceedings

Probabilistic Analysis of the Spatio-Temporal Variability of the Pugllohuma Peatland Using Synthetic Aperture Radar Images of the Sentinel-1 Mission †

Paul David Carchipulla-Morales [1,2,*] and Xavier Eduardo Zapata-Ríos [1,2]

1. Department of Civil and Environmental Engineering, Escuela Politécnica Nacional, Quito 170517, Ecuador
2. Center for Research and Water Resources Studies, Escuela Politécnica Nacional, Quito 170517, Ecuador; cierhi@epn.edu.ec

* Correspondence: paul.carchipulla@epn.edu.ec

† Presented at the 8th International Symposium on Sensor Science, 17–26 May 2021; Available online: https://i3s2021dresden.sciforum.net/.

Published: date

Abstract: This study presents the spatio-temporal assessment of the Pugllohuma peatland's surface variability, a highland wetland (over 4100 m.a.s.l.) in the Sustainable water conservation area Antisana, Ecuador. This assessment provided information of the surface variability during dry and wet season. The temporal variability was investigated through the pressure, rain, relative humidity, temperature, and wind, records of two near meteorological stations, while the spatial variability was investigated through images of the Sentinel-1 mission from 2017 to 2019, as well as, elevation and slope data. Their classifications were carried out by using R programming language and Google Earth Engine, and the results were published in the UI service in Google Apps Script.

Keywords: Sentinel-1; wetland; Google Earth engine; random forest

1. Introduction

The study of environmentally sensitive areas and their ecosystem services is relevant worldwide because of their importance in anthropic interests and activities. The Pugllohuma peatland is in the Mica Quito-Sur system, which is one of the four water collection systems used in Quito, city and capital of Ecuador, and its conservation influences the hydrological cycle of the water that reaches Quito's drinking water network [1]. Commonly, the use of optical images was obstructed by cloud cover and volcanic plumes [2,3]. Therefore, the current research used radar images to detect changes in the peatland's land surface water from 2017 to 2019, and the radar image classification process was developed by decision trees to perform supervised classifications [4,5]. Thereby, the building of supervised classification models showed that Pugllohuma peatland's space-time changes are governed by the day of the year, terrain elevation, atmospheric temperature, and precipitation. So, the soil drought season takes place in January, February, and March, whereas high water tables were frequent from June to September, and from November to December. Finally, the area of interest showed its seasonal changes around the following distribution of the land classes: 170 ha of dry soil, 17 ha of moist soil, and 7 ha of soil near saturation.

2. Materials and Methods

The developed methodology pretended to take advantage of the local weather datasets and the Sentinel-1 imagery for assessing the changes in land surface water of Pugllohuma peatland. Figure 1 shows a flowchart highlighting the key steps and datasets used. This workflow involves three primary steps, which included the use of correlation matrices, plots of OOB errors against number of treess, as well as the Mean Decrease Accuracy and Mean Decrease Gini index to build and assess the classification models.

1. Generation of temporal supervised classification using R Studio.
2. Imagery selection and pre-processing using Google Earth Engine.
3. Generation of spatial supervised classification using Google Earth Engine.

Firstly, the temporal supervised classification was used to classify the extreme dry and wet events in the peatland, based on water table and weather registers [6–8]. Later, the dates of extreme events were used in the imagery selection, which pixel values were correlated to land water, flooded vegetation and roads surfaces. Finally, the backscattering, terrain data and the day of the year of the imagery were used to classify the land variability in the Pugllohuma's peatland from 2017 to 2019 [9].

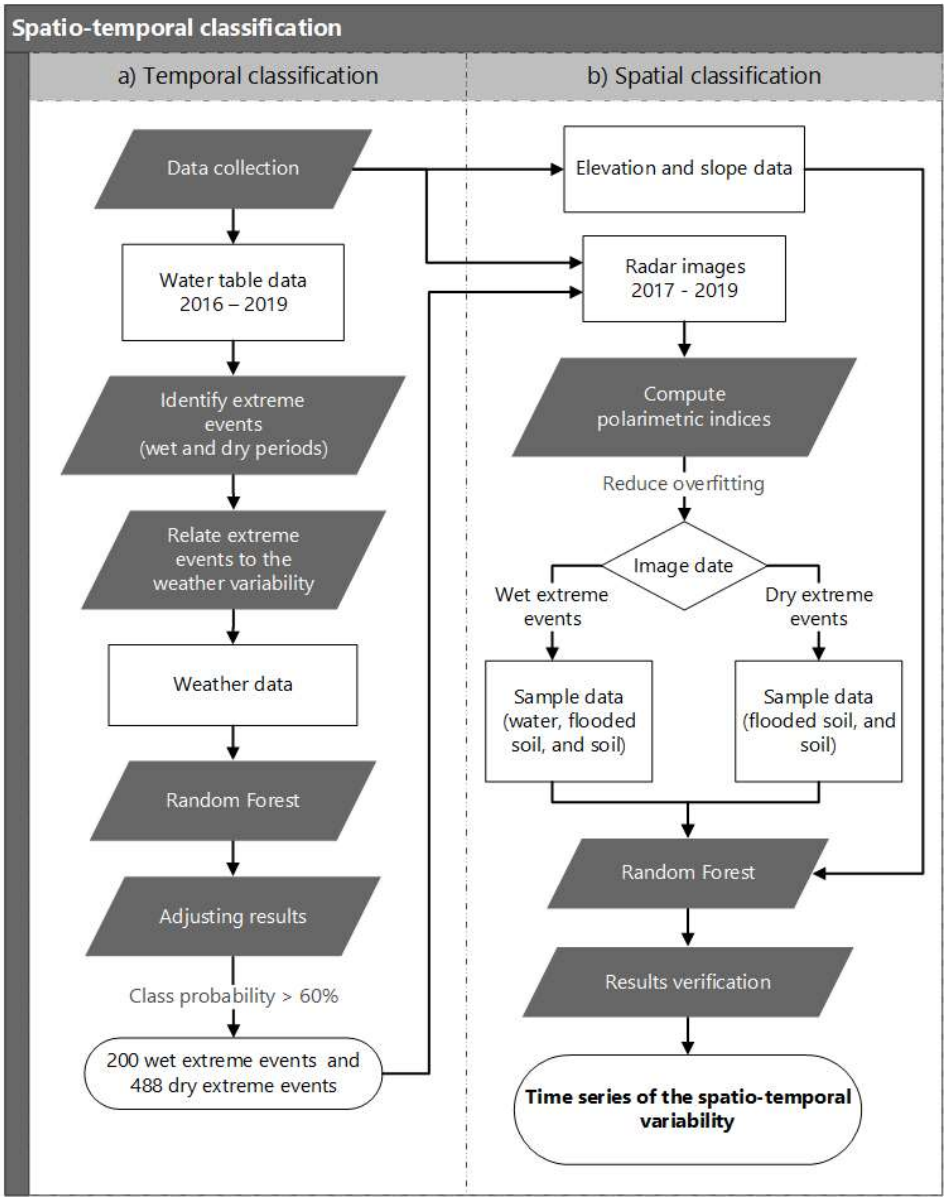

Figure 1. Workflow of Pugllohuma peatland's surface spatio-temporal supervised classification: (**a**) Temporal classification. (**b**) Spatial classification. The parallelograms are used for data, rectangles for activities, diamonds for decisions, and rounded rectangles for products.

3. Results

3.1. Extreme events

While collecting weather samples for the classification, it was observed that wet extreme events occur frequently from April to June and from October to December. Oppositely, the dry extreme events are frequently registered in January, February, July, August, and September. The main variables for identifying extreme events were the day of the year, atmospheric temperature, rain, and elevation of the terrain. In Figure 2, it is observed that the classification results were inconsistent with the seasonality in samples. So, it was preferred to use the results which predicted class probability is above 0.6.

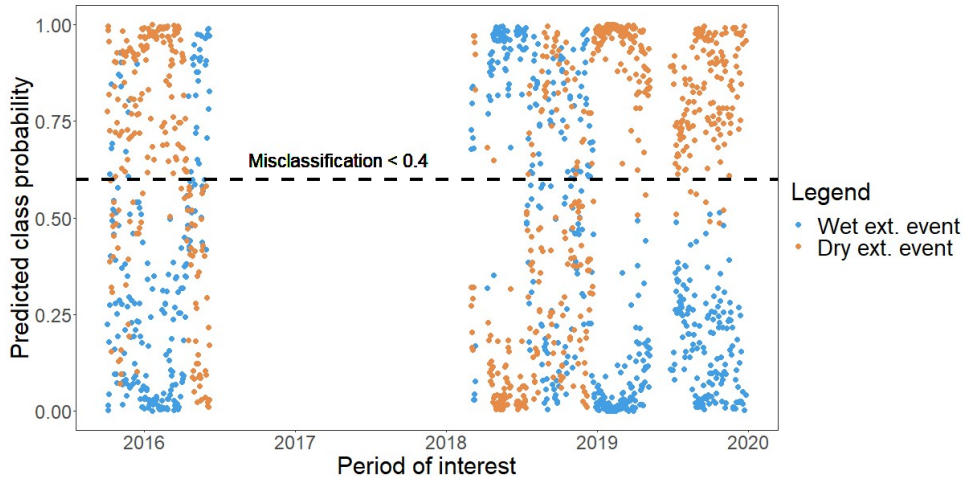

Figure 2. Temporal distribution of the dry and wet events.

3.2. Spatio-temporal classification time series

The temporal variation of the dry and wet soil, as well as the saturated soil, may be observed in Figure 3, Figure 4, and Figure 5, which top events are highlighted in grey. The time series of soil classification show remarkable seasonal variations in dry soil, and less clear seasonal variations in wet and saturated soil. It was discerned that the water presence in the peatland is related to the weather extreme events. Extreme events in the peatland surfaces occurs after weather extreme events. So, the peatland is dry from January, to March, and it is wet from June to September and from November to December. Beside, the time series locate the seasonal changes in the center and south of the wetland, eventual changes in the south of the wetland, and the permanent accumulation of water zones with more vegetation.

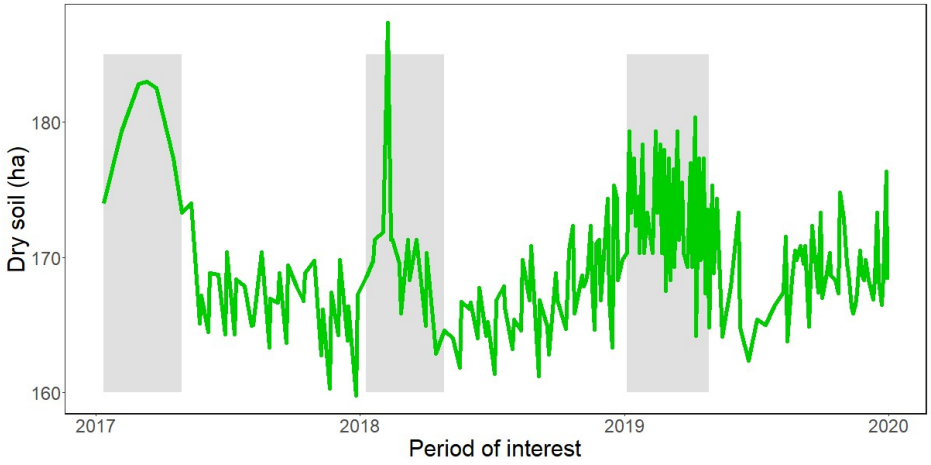

Figure 3. Evolution of the spatio-temporal classification of dry soil.

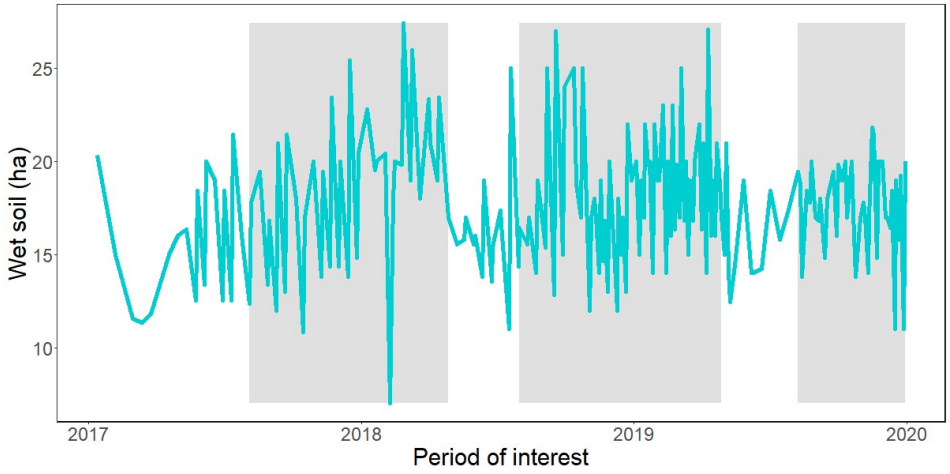

Figure 4. Evolution of the spatio-temporal classification of wet soil.

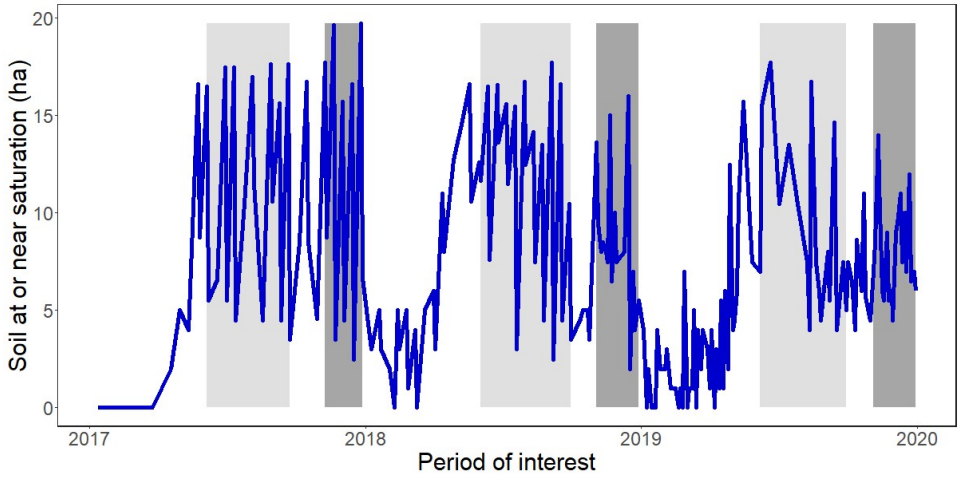

Figure 5. Evolution of the spatio-temporal classification of soil at or near saturation.

3.3. Verifying Results

The comparison between supervised and unsupervised classifications indicates that using radar images is not effective when evaluating the spatial distribution of classes on surfaces smaller than 20

ha due to the correction required for radar images by speckle. Besides, the results of both classifications can be similar in 70 % of the surface. So, the results of the spatio-temporal model have less uncertainty when the peatland is made up of 170 ha of dry soil, 17 ha of moist soil, and 7 ha of soil close to saturation. However, the maps of the supervised classification show sharper boundaries between classes than those presented in the unsupervised classification. The difference between both results denotes the sensitivity of optical sensors to changes in vegetation and the sensitivity of radar sensors to topographic changes due to the water content in the Andean vegetation and soil shapes.

Funding: This research was funded by Escuela Politécnica Nacional under the framework of project PIJ-17-05: Global climatic patterns and their influence on the temporal and spatial response of spectral indices of the paramo vegetation in Ecuador.

Data Availability Statement: The supervised classification results are available at https://pij-17-05.users.earthengine.app/view/sar-landtrendr, and the comparison between both classifications is available at https://pij-17-05.users.earthengine.app/view/landtrendrassessment.

Conflicts of Interest: The authors declare no conflict of interest.

References

1. FONAG. Informe De Cumplimiento De Metas - Plan De Monitoreo 2019. Technical Report, 2019.
2. Schroeder, R.; Rawlins, M.A.; McDonald, K.C.; Podest, E.; Zimmermann, R.; Kueppers, M. Satellite microwave remote sensing of North Eurasian inundation dynamics: Development of coarse-resolution products and comparison with high-resolution synthetic aperture radar data. *Environ. Res. Lett.* **2010**, *5*. doi:10.1088/1748-9326/5/1/015003.
3. Guo, M.; Li, J.; Sheng, C.; Xu, J.; Wu, L. A review of wetland remote sensing. *Sensors* **2017**, *17*, 777. doi:10.3390/s17040777.
4. Huang, W.; DeVries, B.; Huang, C.; Lang, M.W.; Jones, J.W.; Creed, I.F.; Carroll, M.L. Automated extraction of surface water extent from Sentinel-1 data. *Remote Sens.* **2018**, *10*, 797. doi:10.3390/rs10050797.
5. Mahdianpari, M.; Salehi, B.; Mohammadimanesh, F.; Homayouni, S.; Gill, E. The first wetland inventory map of newfoundland at a spatial resolution of 10 m using sentinel-1 and sentinel-2 data on the Google Earth Engine cloud computing platform. *Remote Sens.* **2019**, *11*, 43, doi:10.3390/rs11010043.
6. Taylor, C.J.; Alley, W.M. Ground-water-level monitoring and the importance of long-term water-level data. *US Geol. Surv. Circ.* **2001**, pp. 1–68.
7. Shepherd, T. Measuring water levels in wells. Technical report, Department of Health, Department of Ecology, Tacoma, 2009.
8. Schumacher, J.G.; Klesschulte, M.J. Investigation of a Monitoring Well Completed in the St . Francois Aquifer in Oregon County, Missouri, 2005–08 Scientific Investigations Report 2010–5041 **2010**. p. 22. doi:10.3133/sir20105041.
9. Jensen, K.; McDonald, K.; Podest, E.; Rodriguez-Alvarez, N.; Horna, V.; Steiner, N. Assessing L-Band GNSS-reflectometry and imaging radar for detecting sub-canopy inundation dynamics in a tropicalwetlands complex. *Remote Sens.* **2018**, *10*, 1–29. doi:10.3390/rs10091431